Experimental validation of nonlinear Fourier transform-based Kerr-nonlinearity identification over a 1600km SSMF link

de Koster, P.B.J.; Koch, Jonas; Schulz, Olaf; Pachnicke, Stephan; Wahls, S.

DOI
10.1364/OFC.2022.W2A.39

Publication date
2022

Document Version
Accepted author manuscript

Published in
Proceedings of the Optical Fiber Communications Conference and Exhibition (OFC 2022)

Experimental validation of nonlinear Fourier transform-based Kerr-nonlinearity identification over a 1600 km SSMF link

Pascal de Koster[(1)], Jonas Koch[(2)], Olaf Schulz[(2)], Stephan Pachnicke[(2)], Sander Wahls[(1)]

[(1)] *Delft Center for Systems and Control, Delft University of Technology, Mekelweg 2, Delft, Netherlands*
[(2)] *Chair of Communications, Christian-Albrechts-Universität zu Kiel, Kaiserstrasse 2, Kiel, Germany*
p.b.j.dekoster@tudelft.nl

Abstract: Recently, a nonlinear Fourier transform-based Kerr-nonlinearity identification algorithm was demonstrated for a 1000 km NZDSF link with accuracy of 75%. Here, we demonstrate an accuracy of 99% over 1600 km SSMF. Reasons for improved accuracy are discussed.

1. Introduction

The nonlinear Kerr effect is one of the major effects that limit the achievable data rates in optical communication. While it can be compensated, for example through digital back-propagation [1], nonlinearity compensation requires accurate knowledge of the Kerr-nonlinearity coefficient of the fiber. Often, values from the data sheets of the installed fibers are used. However, the actual Kerr-nonlinearity may be different due to incomplete knowledge of the link or splice losses during installation [2, p.191]. To identify the Kerr-nonlinearity in an installed single mode fiber, commonly the link is simulated with different Kerr coefficients using split-step Fourier methods (SSFM); the coefficient that fits best is kept [3, 4]. However, the number of steps required for the SSFM increases with the link length, and also time- and phase-offsets have to be compensated for the equalization process.

To overcome these drawbacks, an identification method based on matching of the discrete spectra (solitonic components) of the nonlinear Fourier transform (NFT) of input-output data was proposed and validated through simulations in [5]. For a noiseless and lossless link, the solitonic components within the transmitted signal coincide exactly with the solitonic components in the received signal, but only when the correct Kerr-nonlinearity coefficient was used for the normalization step in the nonlinear Fourier transform. The nonlinearity coefficient may thus be determined as the value at which the solitonic components at the transmitter and receiver match optimally. No propagation of the signal is required. Furthermore, time- and phase-offsets do not influence the identification.

First experimental results of the NFT-based nonlinearity identification applied on a non-zero dispersion shifted fiber (NZDSF) in [6] reported an identified nonlinearity coefficient up to 25% higher than the benchmark value obtained using a split-step Fourier method. In this paper, we present experimental results of the NFT-based identification algorithm applied on a standard single-mode fiber (SSMF) that identifies the Kerr-nonlinearity coefficient within 1% of the benchmark value. The pre-processing for the NFT-based algorithm furthermore does not contain any time- or phase-shift compensation in his paper, which experimentally verifies for the first time that the NFT-based method does not require these steps.

2. Nonlinear Fourier transform and identification algorithm

The propagation of a signal through a span of single-mode fiber with anomalous dispersion can be described by a lossy nonlinear Schrödinger equation (NLSE) [2], $A_l = -i\frac{\beta_2}{2}A_{\tau\tau} + i\gamma|A|^2A - \frac{\alpha}{2}A$, where $A(\tau, l)$ is the signal envelope as a function of time τ and distance l. Here, β_2 denotes the second-order dispersion coefficient, γ the Kerr-nonlinearity coefficient, and subscripts partial derivatives. At the end of each span the signal power is amplified by an EDFA to a fixed power level. The NFT-based method requires a lossless NLSE. Therefore, we apply the path-average approximation [7]:

$$Q = Ae^{\alpha l/2}, \quad \gamma_1 = \frac{1}{L_{\text{span}}}\int_0^{L_{\text{span}}} \gamma e^{-\alpha l}\,\mathrm{d}l = \gamma\frac{1-e^{-\alpha L_{\text{span}}}}{\alpha L_{\text{span}}}, \quad \Rightarrow \quad Q_l \approx -i\frac{\beta_2}{2}Q_{\tau\tau} + i\gamma_1|Q|^2Q, \tag{1}$$

where $Q(\tau,l)$ is the loss-compensated amplitude and γ_1 the path-averaged Kerr-nonlinearity coefficient. The NFT is typically computed from the normalized and dimensionless NLSE, so we apply the following normalization [8]:

$$t=\frac{1}{T_0}\tau,\quad q=T_0\underbrace{\sqrt{|\gamma_1/\beta_2|}}_{c_q}Q,\quad z=\frac{1}{T_0^2}\underbrace{(-\beta_2/2)}_{c_z}l\qquad\Rightarrow\qquad q_z=iq_{tt}+2i|q|^2q. \tag{2}$$

Note that the amplitude normalization c_q and space normalization c_z are fixed by β_2 and γ_1, but that the time normalization T_0 is a free parameter (similar to the linear Fourier transform, it simply re-scales the spectrum). As the choice of T_0 does not influence any further analysis, we set $T_0=1$ s.

The NFT of a normalized signal $q(t)$ with vanishing boundary conditions is defined as follows [1]:

$$\frac{d}{dt}\begin{bmatrix}\phi_1(t,\lambda)\\ \phi_2(t,\lambda)\end{bmatrix}=\begin{bmatrix}-i\lambda & q(t)\\ -q^*(t) & i\lambda\end{bmatrix}\begin{bmatrix}\phi_1(t,\lambda)\\ \phi_2(t,\lambda)\end{bmatrix},\qquad\begin{bmatrix}e^{-i\lambda t}\\ 0\end{bmatrix}\overset{t\to-\infty}{\longleftarrow}\begin{bmatrix}\phi_1(t,\lambda)\\ \phi_2(t,\lambda)\end{bmatrix}\overset{t\to+\infty}{\longrightarrow}\begin{bmatrix}a(\lambda)e^{-i\lambda t}\\ b(\lambda)e^{+i\lambda t}\end{bmatrix}. \tag{3}$$

The NFT spectrum consists of two parts: the discrete spectrum $\{(\lambda_k,b(\lambda_k)):a(\lambda_k)=0,\Im(\lambda_k)>0\}$ represents solitonic components; the continuous spectrum $\{b(\xi):\xi\in\mathbb{R}\}$ represents dispersive components. Assuming that the signal propagates exactly according to the normalized NLSE, both the eigenvalues λ_k and the amplitudes of the continuous spectrum $|b(\xi)|$ remain constant [1]. We only consider the eigenvalues λ_k of the discrete spectrum in this paper, as we observed that the continuous spectrum contains only a small part ($<5\%$) of the energy for the used signals. We finally recall that the eigenvalues are invariant under time- and phase-offsets of the signal [8, p.4319].

The NFT-based identification algorithm is based on [5] and has the following steps: 1) a c_q is selected from a grid for the normalization; 2) the eigenvalues of the transmitted and received signal are determined from the normalized signals; 3) the matching error E is determined as follows:

$$E=\min_{m(k)}\frac{\sum_k E_{km(k)}}{\sum_k\Im\left(\lambda_k^{\text{in}}\right)+\sum_m\Im\left(\lambda_m^{\text{out}}\right)},\quad\text{with}\quad E_{km}=\min\left(|\lambda_m^{\text{out}}-\lambda_k^{\text{in}}|,\Im(\lambda_k^{\text{in}}+\lambda_m^{\text{out}})\right), \tag{4}$$

where $m(k)$ denotes the perfect matching which connects input eigenvalue λ_k^{in} to output eigenvalue λ_m^{out}, and E_{km} the cost of connecting these eigenvalues. In case the input and output spectra have different numbers of eigenvalues, unmatched eigenvalues of the larger spectrum are assigned a maximum cost: $E_{k-}=\Im\left(\lambda_k^{\text{in}}\right)$, $E_{-m}=\Im\left(\lambda_m^{\text{out}}\right)$. An exemplary matching at optimal c_q of one of the used signals is shown in Fig. 2a. The steps 1)-3) are repeated for every grid point. The c_q with the lowest error is then used to recover γ using Eqs. 1 and 2. This procedure is performed for each signal block, and all estimates for γ are averaged for a final estimate.

3. Experimental results

The used setup is shown in Fig. 1. One hundred blocks of 128 QPSK symbols with a symbol rate of 10 GBd (burst length 12.8 ns) were transmitted with guard intervals of 3.2 ns between consecutive blocks. A raised cosine filter with roll-off factor 0.5 was used for pulse shaping. The digital signal was pre-compensated for the measured frequency response of the back-to-back transceiver setup. Digital to analogue conversion was done using an 88 GS/s arbitrary waveform generator (AWG). The analogue signal was converted into the optical domain at 1550 nm carrier wavelength using an I/Q modulator and a laser with $<$100 kHz linewidth. The optical signal was amplified to 2 dBm launch power before every fiber span, and circulated 8 times through a loop of 4 spans of 50 km OFS AllWave SMF for a total of 1600 km. The reference fiber coefficients for α and β_2 were taken from the data sheet. However, γ was not provided, so we used a typical value from the literature [9, p.157]: $\beta_2^{\text{ref}}=-21.2\frac{\text{fs}^2}{\text{m}}(D=16.6\frac{\text{ps}}{\text{nm}\cdot\text{km}})$, $\alpha^{\text{ref}}=0.19\frac{\text{dB}}{\text{km}}$, $\gamma^{\text{ref}}=1.26\frac{1}{\text{Wkm}}$. After polarization de-rotation, the signal was received using a $<$10 kHz linewidth laser and an 80 GS/s coherent receiver. Finally, the signal was post-processed as indicated in Fig. 1.

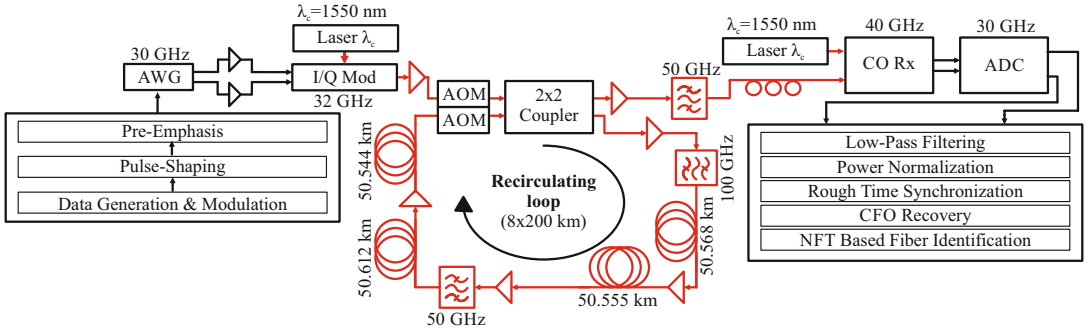

Fig. 1: The used setup with exact fiber lengths, positions of optical filters, and applied signal-processing.

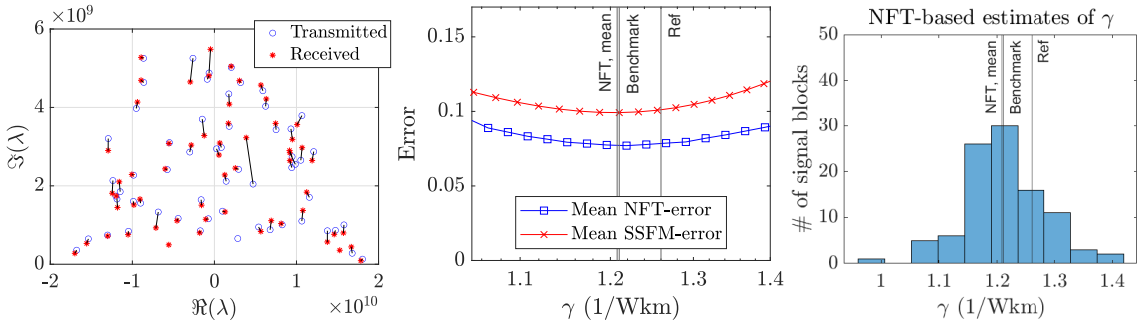

(a) (b) (c)

Fig. 2: (a) The matching of detected eigenvalues at transmitter and receiver at optimal normalization of a single signal block. (b) The average discrete spectrum error over 100 individual blocks, compared to the SSFM-error of the full 100-block signal. (c) The NFT-based estimates of γ for each of the 100 blocks of input-output data, along with the mean of the NFT-based estimates and the benchmark value.

To convert c_q from the NFT-based method to γ with Eqs. 1 and 2, we require β_2 precisely. We identified it by comparing the phase shifts in the linear Fourier spectrum of the full signal of 100 blocks at the transmitter and receiver, and found $\beta_2^{\mathrm{ID}} = -20.6\frac{\mathrm{fs}^2}{\mathrm{m}}$ ($D = 16.2\frac{\mathrm{ps}}{\mathrm{nm\cdot km}}$). We identified γ using the NFT method and the benchmark using the SSFM as described in the previous section. For both the SSFM method and for the conversion from c_q to γ in the NFT method, we used $\beta_2 = \beta_2^{\mathrm{ID}}$, $\alpha = \alpha^{\mathrm{ref}}$ and the mean span length.

The results are presented in Figs. 2b and 2c. The mean of the identified values for γ^{NFT} ($= 1.207\frac{1}{\mathrm{Wkm}}$) from the NFT-based method is within 1% of the benchmark method ($\gamma^{\mathrm{benchmark}} = 1.1210\frac{1}{\mathrm{Wkm}}$), which are both slightly lower than the reference value ($\gamma^{\mathrm{ref}} = 1.26\frac{1}{\mathrm{Wkm}}$). In contrast to the 25% difference in [6], the NFT-based value for γ is nearly identical to the benchmark method. While the fiber in [6] was different, we think that the difference is likely reduced because we hand-tuned the Mach-Zehnder modulators to prevent non-zero means in the optical offset and remeasured the frequency response of the transceiver that is used for linear pre-compensation. Finally, the method used for the benchmark value in [6] contained a subtle conceptual mistake in the phase-offset correction step, that biased the identified γ towards the reference value.

4. Conclusion

We validated the effectiveness of nonlinear Fourier transform-based Kerr-nonlinearity identification on experimental fiber-optical transmission data, without employing time- and phase-offset compensation. The identified nonlinearity coefficient obtained with the nonlinear Fourier transform was within 1% of the benchmark value using the split-step Fourier method. Future research will investigate speeding up the NFT-based method, for example by identifying and matching only the highest few eigenvalues.

References

1. S. K. Turitsyn, J. E. Prilepsky, S. T. Le, S. Wahls, L. L. Frumin, M. Kamalian, and S. A. Derevyanko, "Nonlinear Fourier transform for optical data processing and transmission: advances and perspectives," Optica **4**, 307–322 (2017).
2. G. P. Agrawal, *Fiber-optic communication systems* (John Wiley & Sons, 2012).
3. M. Piels, E. P. da Silva, D. Zibar, and R. Borkowski, "Performance emulation and parameter estimation for nonlinear fibre-optic links," in *2016 21st European Conference on Networks and Optical Communications (NOC),* (IEEE, 2016), pp. 1–5.
4. L. Jiang, L. Yan, A. Yi, Y. Pan, M. Hao, W. Pan, B. Luo, and Y. Jaouën, "Chromatic dispersion, nonlinear parameter, and modulation format monitoring based on Godard's error for coherent optical transmission systems," IEEE Photonics J. **10**, 1–12 (2018).
5. P. de Koster and S. Wahls, "Dispersion and nonlinearity identification for single-mode fibers using the nonlinear Fourier transform," J. Light. Technol. **38**, 3252–3260 (2020).
6. P. de Koster, J. Koch, S. Pachnicke, and S. Wahls, "Experimental investigation of nonlinear Fourier transform based fibre nonlinearity characterisation," in *47th European Conference on Optical Communication (ECOC 2021),* (2021).
7. S. T. Le, J. E. Prilepsky, and S. K. Turitsyn, "Nonlinear inverse synthesis technique for optical links with lumped amplification," Opt. express **23**, 8317–8328 (2015).
8. M. I. Yousefi and F. R. Kschischang, "Information transmission using the nonlinear Fourier transform, part I: Mathematical tools," IEEE Transactions on Inf. Theory **60**, 4312–4328 (2014).
9. S. Pachnicke, *Fiber-optic transmission networks: efficient design and dynamic operation* (Springer, 2011).